

Adsorption of an alkane mixture on carbon nanotubes: Selectivity and kinetics

Chenyu Wei*

NASA Ames Research Center, MS 229-1, Moffett Field, California 94035, USA

(Received 18 May 2009; revised manuscript received 19 July 2009; published 10 August 2009)

Adsorption and its dynamical process of polymer mixtures consisting of long and short alkane molecules around a carbon nanotube (CNT) are studied with molecular-dynamics (MD) simulations and master equation. Preferred adsorption is found for long chained molecules compared to short ones, due to favorable interfacial interaction energies of the former with the tube. A dominating ratio ~ 32 is calculated for the adsorption sites of heptane molecules vs decane molecules in their equal weight melt mixture when around a CNT (5, 5) at 420 K. The adsorption-desorption kinetics of the molecules is described through a master equation in combination with MD simulations. A fully adsorbed alkane molecule is found to be much more stable than a partially adsorbed one, regarding its monomer desorption rate from the nanotube. This results in a sharp peak in the population of the morphology of the adsorbed molecules at their maximum bound fraction $f_b=1$. The crystallization in the mixture composite and the selectivity and molecule morphology during a cooling process were also discussed.

DOI: [10.1103/PhysRevB.80.085409](https://doi.org/10.1103/PhysRevB.80.085409)

PACS number(s): 68.08.-p, 64.70.Nd, 61.30.-v

I. INTRODUCTION

Carbon nanotubes (CNTs) have been recently investigated as additive fibers for multifunctional nanocomposites and as sensors for polymer or biopolymer molecules to take advantages of CNTs' high strength and thermal conductivity and structure and environment sensitive electronic properties.¹ Polymeric CNT composites have been studied extensively due to their vast applications.² A general issue in these nanocomposites, similarly as in traditional polymer composites, is that there usually is a broad dispersity in the chain lengths of the matrix molecules.³ This dispersity can greatly influence the properties of a composite such as load transfers and thermal coupling or in its lubrication and coating applications, due to length-dependent molecular adsorptions and morphologies at the interface. The properties of bulk polymer matrix can be affected subsequently also, as shown in recent experiments, where the favorable adsorption of long polyethylene (PE) molecules over short ones around CNTs was suggested to contribute to a drop of the viscosity of its CNT composites⁴ and silica nanoparticle composites.⁵

In this study we investigate the competing and dynamical adsorption process of a binary polymer (alkane) mixture consisting of long and short chains around a CNT with molecular-dynamics (MD) simulations.⁶ MD simulations can provide atomic-level descriptions for the interfacial interactions, which is vital for the understandings of the conformations of adsorbed molecules on a CNT, as shown in numerous experimental, modeling, and theoretical studies on structural ordering and assembly and radius-dependent and chirality-dependent adsorptions of polymer⁷⁻⁹ or DNA molecules.¹⁰ In this study, besides selective adsorptions in the mixture, we also investigate the adsorption-desorption kinetics and the morphology of the alkane molecules on the CNT. A master equation was used to understand the competing adsorption process, in combination with the MD simulations.

II. SIMULATION METHOD

An united atom force field was used for the alkane molecules, which includes bond-stretching, angle-bending, and

dihedral angle-rotation terms. AMBER force field¹¹ was used for the CNT. Truncated 6–12-typed Lennard-Jones potentials were used for the van der Waals (VDW) interactions between the alkane molecules or any two segments separated by more than four units within a molecule and with the CNT. The details of the force fields can be found elsewhere.¹² The representing mixture system considered in this study consists of 40 heptane ($C_{10}H_{22}$) and 400 decane ($C_{10}H_{22}$) molecules embedded with a continuous CNT (5, 5) (~ 200 Å) in a periodic unit cell with size about $40 \times 40 \times 200$ Å. Each individual alkane molecule was relaxed with a Monte Carlo (MC) simulation up to two million steps¹² such that the end-to-end distance of the molecule shows the square-root dependence on the chain length as predicted by Flory's theory.¹³ After the MC relaxations, the molecules were put together with random translational and orientational positions around the CNT. Anisotropic Berendsen NPT ensemble with $P=1$ kbar was used with thermostat and barostat relaxation time at 0.5 and 1.5 ps, respectively (applied to all the atoms). A time step of 1 fs was used. To study the dynamical process of the molecule adsorption within the time scale of the MD simulations (tens of nanoseconds), a temperature of $T=420$ K was set, which is above the glass transition temperature of $T_g \sim 289$ K (estimated from density vs temperature plot). At $T=420$ K, the heptane-decane mixture is in a melt state. Other binary mixture system with less dramatic difference in their chain lengths, such as eicosane ($C_{20}H_{42}$) and decane, were also investigated.

III. RESULTS AND DISCUSSIONS**A. Selective adsorptions in the mixture at the CNT surface**

Starting from the initial condition that the heptane and decane molecules were distributed randomly around the CNT (5, 5), a much more preferred adsorption of the long chained $C_{10}H_{22}$ molecules over the $C_{10}H_{22}$ molecules is found during equilibrium MD simulations up to 10 ns, with the decane molecules depleting from the nanotube surface

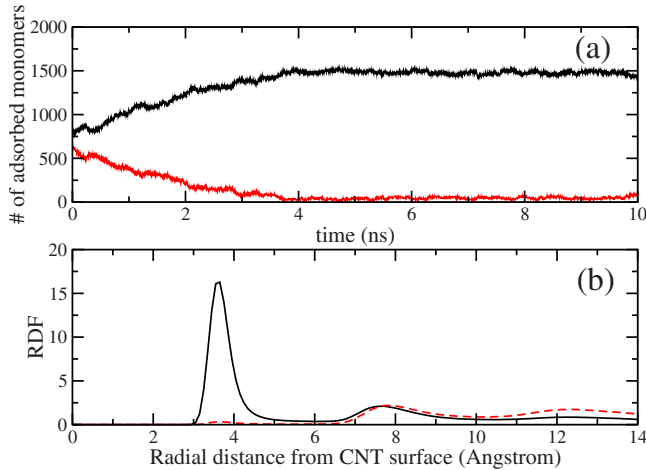


FIG. 1. (Color online) (a) The number of adsorbed monomers for the heptane (black upper curve) and decane [red (dark gray) lower curve] molecules as a function of time. (b) The RDF for the heptane (black solid curve) and decane [red (dark gray) dashed curve] molecules in the CNT (5, 5) mixture composite (averaged over the last 5 ns simulations).

and replaced by the heptane molecules. Such process is shown in Fig. 1(a), in which the number of the adsorbed monomers, n_h for the heptane molecules and n_d for decane molecules, is plotted as a function of time. A monomer is considered to be adsorbed directly on the CNT, if its radial distance to the tube surface < 6 Å within the first adsorption layer [see Fig. 1(b)]. It can be seen that starting from the rather close values with $n_h \sim 772$ and $n_d \sim 620$ at $t=0$, the number of the adsorbed monomers for heptane increases up to a stable value of $n_h \sim 1478$, accompanied by the decreasing of n_d down to ~ 46 , after 4 ns simulation runs. The radial distribution function (RDF) for the heptane and decane molecules from the tube surface is shown in Fig. 1(b), with a much enhanced peak for the former in the first layer (the RDF values are averaged over the last 5 ns simulations). As an illustration, the configurations of the heptane-decane system at an early time ($t=80$ ps) and at $t=10$ ns are shown in Fig. 2 in comparison (only monomers in the first adsorption layer are shown). The adsorbed molecules or the segments of a partially adsorbed one has their orientations predominately along the CNT (5, 5) axis, which is due to the optimal interaction energies with the nanotube lattice and the minimized molecule bending energy around the armchaired tube with small radius.⁸ The molecule orientation feature appears at early times [see Fig. 2(b)], suggesting that the aligning process is fast in the melt mixture.

The total number of the adsorbed monomers is roughly constant at $n_t = n_h + n_d \sim 1525$, suggesting a saturated adsorption surface. There is a slight increase in n_t during the initial 4 ns simulation, due to the improved molecule packing arrangements at the tube surface. A coverage ratio of 0.9 is obtained for this alkane mixture, considering the lattice site of 1700 on the CNT (5, 5) in the simulation. In comparison, a smaller coverage ratio of 0.8 is found for a same weight but pure decane matrix around the same length CNT (5, 5), with its $n_t \sim 1360$ compared to that of 1525 in the heptane-decane mixture. This fact supports the consideration that the pre-

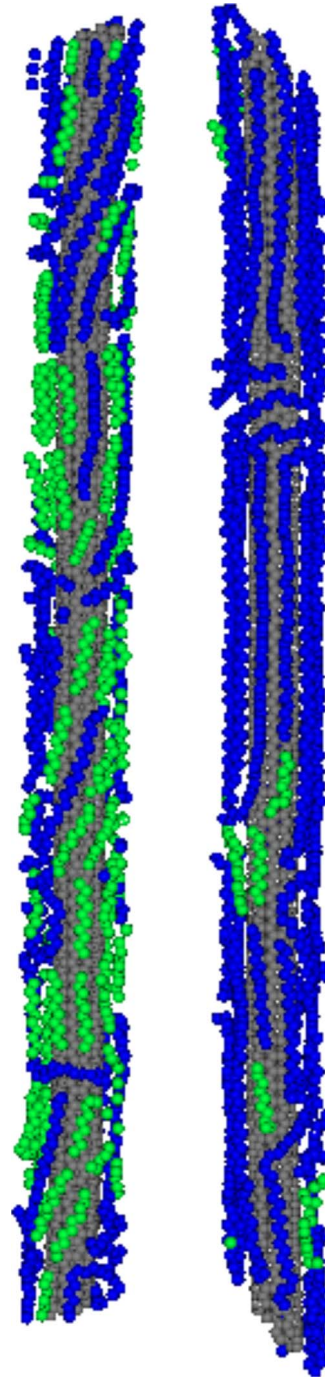


FIG. 2. (Color online) The configuration plot for the adsorbed monomers on the CNT (5,5) surface. Left: $t=80$ ps; right: $t=10$ ns. Light gray: nanotube; green (gray): decane; blue (dark gray): heptane. Atoms outside the first adsorption layer are not shown.

ferred adsorption of the longer alkane molecules over the shorter ones is due to energetic reasons. When the alkane molecules adsorb on a surface, the intermolecule distance, which needs to be in the range of the VDW distance ~ 4 Å, is much larger than the intramolecule C-C bond length (~ 1.5 Å). So the shorter molecules would have more end units compared to the longer ones, which results in more adsorption sites and thus preferred adsorptions for the longer

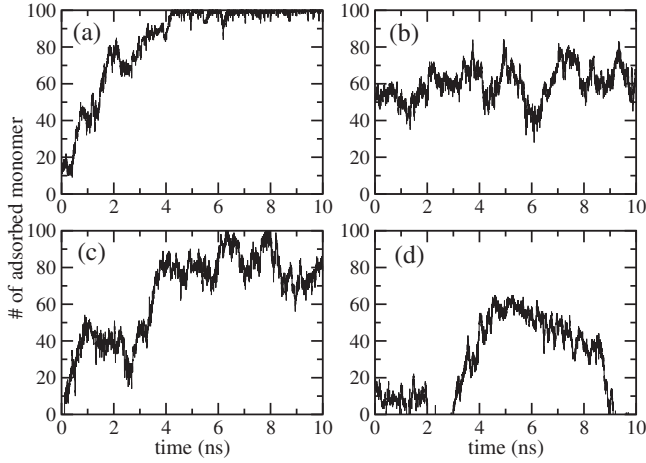


FIG. 3. The number of the adsorbed monomers of an individual heptane molecule as a function of time [four selected cases shown in (a)–(d)].

chains. An eicosane ($C_{20}H_{42}$)-decane mixture (200 eicosane and 400 decane molecules) with a less dramatic comparison in their chain lengths (ratio=2) was also simulated for 10 ns at $T=300$ K, and a preferred adsorption of the $C_{20}H_{42}$ over the $C_{10}H_{22}$ molecules was also found around the CNT (5, 5) but with a much less dominating ratio ($\sim 1136/320 \approx 3$), compared to that of $n_b/n_d \sim 1478/46 \approx 32$ for the heptane-decane mixture. This difference is consistent with the above energetic consideration based on the chain lengths. The total number of the adsorbed monomers on the tube surface in the eicosane-decane mixture is 1456, which is less compared to that of 1525 in the heptane-decane mixture. While the entropy lost due to the confinement of the alkane molecules at the tube surface is a competing factor to the adsorption interaction energy, the later is the dominating one as shown from the simulations.

Preferred adsorptions of long chained molecule over short ones have been observed in various systems in both experimental studies,³ including alkane molecules on graphite^{14,15} and simulation studies, such as alkane mixture on Au surface¹⁶ and inside a nanoporous zeolite.¹⁷ A recent experimental study on PE CNT composites also suggested a favorable adsorption of higher molar mass PE component on the tubes.⁴ Groszek¹⁸ had observed selective adsorption of hydrocarbons on graphite, favoring long chain molecules, and the denser adsorption sites for the longer hydrocarbon molecules were also suggested to contribute to the observed preferred adsorption.

B. Kinetics of the competitive adsorption and molecule morphology at the CNT surface

In the melt state of the heptane-decane binary mixture at $T=420$ K, the alkane molecules at the CNT surface frequently exchange and compete for adsorption sites with surrounding molecules, by the process of desorbing and re-adsorbing of monomers. Such dynamical process is still abundant after the number of the adsorbed monomers for both the heptane and decane molecules reaches their stable

values. Shown in Fig. 3 is the number of the adsorbed monomers for an individual heptane molecule as a function of time. Several representing cases were selected: (1) progressive adsorption of a heptane molecule to its fully adsorbed state [Fig. 3(a)]; (2) detaching of an adsorbed chain [Fig. 3(d)]; and (3) two partially adsorbed chains with frequent desorption and adsorption of their monomers from the tube surface [Figs. 3(b) and 3(c)]. The desorption and adsorption process is by one monomer at a time. Peeling off a molecule all at once would have a prohibited high barrier $\sim N \times E_b$ for a N -unit molecule with $N \gg 1$,¹⁹ where E_b is the monomer activation barrier for the detachment. The length dependence and the dynamics of the desorption of a polymer molecule from a solid surface have been investigated in both experiment^{20–22} and simulation studies,^{23,24} which mainly focused on the detachment of a whole molecule chain from a surface and broad distributions in the morphology of adsorbed polymer molecules on a solid surface was suggested from the experimentally observed nonlinear dependence of the desorption barrier on the molecule chain length.^{21,22}

The morphology of the adsorbed molecules on the CNT surface has a wide distribution. To describe their conformations in quantitative details, a bound fraction $f_b = m/N_p$ ($0 < f_b \leq 1$) is defined for a N_p -unit molecule, where m is the number of its adsorbed monomers on the nanotube. The case with $f_b = 1$ represents a fully adsorbed state. To describe the distribution of f_b among all the adsorbed molecules, a time-dependent probability function $P_b(m, t)$ is defined as

$$P_b(m, t) = \langle n_b(m, t) \rangle / \langle N_t(t) \rangle, \quad (1)$$

where $n_b(m, t)$ is the number of the adsorbed molecules with bound fraction m/N_p , $N_t(t)$ is the total number of the adsorbed molecules, and $\langle \rangle$ represents ensemble averages. Considering the desorption and adsorption is through a monomer by monomer process, a master equation can be written for the evolving of the function $n_b(m, t)$ by a small time step Δt ,

$$n_b(m, t + \Delta t) = n_b(m, t)[1 - k^- \Delta t - k^+ \Delta t] + n_b(m + 1, t)k^- \Delta t + n_b(m - 1, t)k^+ \Delta t, \quad (2)$$

where k^- and k^+ is the rate for a monomer desorbing from and adsorbing onto the CNT surface, respectively. Equation (2) can be written in its differential equation form with $\Delta t \rightarrow 0$,

$$\frac{\partial n_b(m, t)}{\partial t} = [n_b(m + 1, t) - n_b(m, t)]k^- + [n_b(m - 1, t) - n_b(m, t)]k^+. \quad (3)$$

For the equilibrium state, with $\lim_{t \rightarrow \infty} \langle N_t(t) \rangle = \text{const.}$ and taking Eq. (1), Eq. (3) can be rewritten as

$$\lim_{t \rightarrow \infty} \frac{\partial P_b(m, t)}{\partial t} = [P_b(m + 1, t) - P_b(m, t)]k^- + [P_b(m - 1, t) - P_b(m, t)]k^+. \quad (4)$$

Take $\lim_{t \rightarrow \infty} \frac{\partial P_b(m, t)}{\partial t} = 0$ and $P_b(m) = \lim_{t \rightarrow \infty} P_b(m, t)$, Eq. (4) is further expressed as

$$P_b(m)[k^- + k^+] = P_b(m+1)k^- + P_b(m-1)k^+. \quad (5)$$

While the above equation holds for the cases for $1 < m < N_p$, special attentions are needed when $m = N_p$ and $m = 1$, which represents the cases for the maximum and minimum monomers possibly adsorbed for a molecule on the tube, respectively. For $m = N_p$,

$$P_b(N_p)[k_s^- + k^+] = P_b(N_p - 1)k^-, \quad (6)$$

where k_s^- is the desorption rate of a monomer for a fully adsorbed molecule (the reason for its introduction will be discussed later). For $m = 1$,

$$P_b(1)[k_s^- + k^+] = P_b(2)k^- + P_0k_0, \quad (7)$$

where P_0 is the probability for an adsorption site available for a new molecule to adsorb on the tube surface and k_0 is the monomer adsorption rate for the molecule. The solutions to Eqs. (5)–(7) are,

$$P_b(m-1) = P_b(m) \frac{k^-}{k^+}, \quad (8)$$

for $m < N_p$, and

$$P_b(N_p-1) = P_b(N_p) \frac{k_s^-}{k^+}, \quad (9)$$

for $m = N_p$ while Eq. (7) implies that $P_b(1)k^- = P_0k_0$. Above master equation and its solution hold for each component of a mixture system.

Detailed analysis on the data from the MD simulations shows that $k^- \approx k^+$ for an adsorbed alkane molecule, with $k^+ \sim 5.14 \text{ ps}^{-1}$ and $k^- \sim 5.07 \text{ ps}^{-1}$ (excluding the desorption events from fully adsorbed molecules). This is not surprising since the adsorption layer is in a saturating state; for a molecule to adsorb one more monomer, an available site must be provided by the desorption of a monomer from its neighboring molecules and once such site is available, the adsorption of the monomer is immediate. With the approximation of $k^+ = k^-$, $P_b(m-1) = P_b(m)$ is expected from Eq. (8) for $m < N_p$, suggesting a flat distribution in P_b .

Shown in Fig. 4 is the calculated probability function P_b , from the MD simulations. At the initial time [red (dark gray) dashed curve] the heptane molecules were in lightly adsorbed states with their f_b s mostly distributed in small values and with the progressing of the adsorptions, the distribution for large $f_b > 0.7$ becomes abundant. After the system reached equilibrium, the P_b (black solid curve) has a flat distribution, except a sharp peak at $f_b = 1$, which represents the fully adsorbed state. The feature of $P_b \sim \text{const.}$ (with thermal fluctuations) for $f_b < 1$ is in agreement with the solutions from the master equation as discussed above. The sharp peak at $f_b = 1$ suggests a much more stable bound state for a fully adsorbed molecule than the partially adsorbed one, which is due to the fact that the later has tails or loops away from the tube surface that would entangle with outer layer molecules, and the corresponding interactions would diminish the stability of the bound portion of the partially adsorbed molecule, thus lower its monomer desorption barrier, compared with the fully adsorbed one.

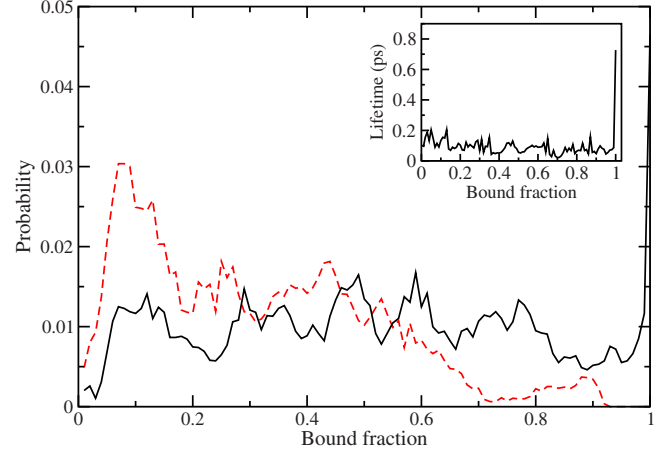


FIG. 4. (Color online) The probability function P_b for the adsorbed heptane molecules in the mixture system. The red (dark gray) dashed and black solid curve is for $t=0$ and 10 ns , respectively. The data was averaged over a 1 ns period. Inset: lifetime of an adsorbed heptane molecule as a function of the bound fraction.

To understand its stability, the lifetime τ of an alkane molecule with bound fraction f_b is defined as the time it spends on the tube surface before the desorption or adsorption of an extra monomer takes place. For $f_b < 1$, the values of τ are in a narrow range with their average $\sim 0.1 \text{ ps}$ for the heptane molecules while an order-of-magnitude larger $\tau_s \sim 0.73 \text{ ps}$ is found for a fully adsorbed one (see the inset of Fig. 4). The ratio between the transition rates k^- and k_s^- is related to the lifetimes as k^-/k_s^- or $k^+/k_s^- = \tau_s/2\tau \sim 3.7$, which gives $P_b(N_p) \sim 3.7 \times P_b(m \neq N_p)$, according to Eq. (9). This is consistent with the ratio ~ 4 of the peak value at $f_b = 1$ vs the averaged value for $f_b < 1$, as shown in Fig. 4 (see the solid curve). The decane molecules have similar values and features in their lifetime and P_b , though there is only a few adsorbed $\text{C}_{10}\text{H}_{22}$ molecules in the equilibrium state. As the desorption process is barrier limited, the ratio between k^- and k_s^- would depend on the temperature as $k^-/k_s^- \sim e^{\Delta E_b/k_B T}$, where $\Delta E_b > 0$ is the difference between the monomer desorption barrier for a fully adsorbed molecule and a partially adsorbed one. At low Ts, it is expected that $k^- \gg k_s^-$ and fully adsorbed molecules would dominate. Such preference is expected to be a general feature for a chain molecule, though the value of k^-/k_s^- and ΔE_b would be system dependent. The ΔE_b is estimated $\sim 0.05 \text{ eV}$ for the alkane molecules studied here.

It should be noted that one of the most important aspects in the polymer adsorption dynamics on a surface is the involved time scale. Slow dynamics is expected for heavy-weighted polymer molecules,²⁵ especially for strong adsorptions, where nonequilibrium²⁶ or even irreversible process²⁷ may be found. A bimodal distribution with a peak at a high bound fraction state for poly (methyl methacrylate) molecules adsorbed on silicon was shown experimentally,²⁶ though nonequilibrium effects were attributed to such observation. For the case in this study, an elevated temperature was used to facilitate the thermal equilibrium of the system and the distribution peak at $f_b = 1$ was due to the higher desorption barrier for monomers in a fully adsorbed alkane molecule.

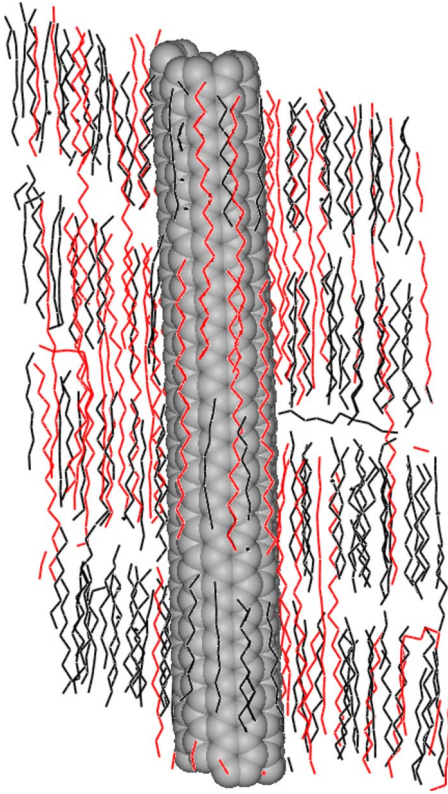


FIG. 5. (Color online) The configuration of the mixture composite of $C_{10}H_{22}$ and $C_{20}H_{42}$ with a CNT (5, 5) at $T=300$ K after an extended 10 ns relaxation following the cooling process. Light Gray: CNT; black: $C_{10}H_{22}$; red (dark gray): $C_{20}H_{42}$. (Portion of the composite shown.)

C. Crystallization in the mixture composite

While above studies mainly concentrate on the adsorption dynamics on the CNT surface, further MD simulations also show that with a gradual cooling process, the mixture of the alkane molecules undergoes a structural phase transition with lamellar layers formed around the CNT that serves as a nucleation site, similarly as that in a single-component alkane CNT composite that was shown in previous modeling studies.²⁸ Two mixture systems were studied: (1) a mixture of 400 $C_{10}H_{22}$ and 200 $C_{20}H_{42}$ molecules embedded with a ~ 200 Å CNT (5, 5); (2) a larger mixture of 1020 $C_{10}H_{22}$ and 102 $C_{100}H_{202}$ molecules embedded with a longer CNT (5, 5) ~ 400 Å. Both mixture composites were prepared at a high temperature of 600 K, with each alkane molecule pre-equilibrated with MC simulations, as described in Sec. II, before putting together in random translational positions and rotational directions. The systems were cooled down from 600 to 300 K with a rate of 10 K/100 ps, and extended relaxations up to 10 and 16 ns were further run at $T=300$ K. The complications in the mixture composite, compared to the single-component alkane CNT composite, is that the longer chained molecule such as $C_{20}H_{42}$ can extend through two lamellar layers that formed by the shorter $C_{10}H_{22}$ molecules, as shown in Fig. 5. The even longer molecule such as $C_{100}H_{202}$ can be in a self-folded configuration to accommodate in the lamellar layers by the $C_{10}H_{22}$ mol-

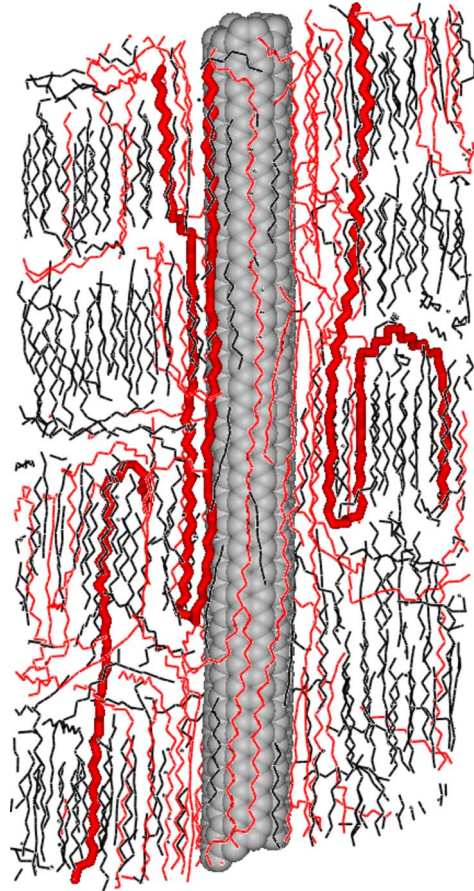


FIG. 6. (Color online) The configuration of the mixture composite of $C_{10}H_{22}$ and $C_{100}H_{202}$ with a CNT (5, 5) at $T=300$ K after an extended 16 ns relaxation following the cooling process. Light gray: CNT; black: $C_{10}H_{22}$; red (dark gray): $C_{100}H_{202}$. Several $C_{100}H_{202}$ molecules that in an self-folded state are marked with stick representation [thick red (dark gray)]. (Portion of the composite shown.)

ecules, as shown in Fig. 6 [see the $C_{100}H_{202}$ molecules marked with stick representation in thick red (dark gray)].

The favorable adsorption of longer chained molecules over the short ones present during the entire cooling process as shown in Fig. 7, where the number of the adsorbed monomers for both the $C_{20}H_{42}$ and $C_{10}H_{22}$ molecules are plotted. Increased selectivity of the former and increased total number of the adsorbed monomers are shown with the decreasing of T . This feature can be contributed to the enhanced energetic contribution compared to the decreased entropy contribution to the adsorption free energy at the lower temperatures, which would favor longer chained molecules further. The uniform feature in the probability function P_b with a sharp peak at $f_b=1$ also presents during the cooling process, as shown in Fig. 8, with an increased ratio between the values of P_b at $f_b=1$ and $f_b < 1$, when T is decreased. In the crystallization state of the composite at $T=300$ K, both the adsorbed $C_{20}H_{42}$ and $C_{10}H_{22}$ molecules' configurations dominate in the fully adsorbed state (see the dash-dotted curve in Fig. 8). Such domination is due to the fact that $k^- \gg k_s^-$ at low temperatures as discussed above.

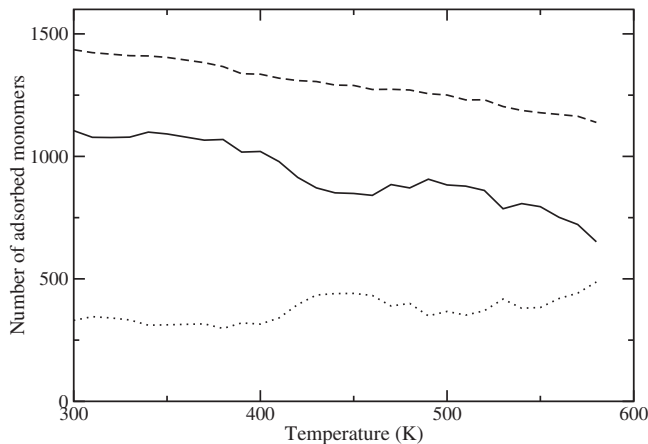


FIG. 7. The number of the adsorbed monomers at the CNT (5, 5) surface in the eicosane-decane mixture composite as a function of temperature during the cooling process. Solid and dotted curve is for the $C_{20}H_{42}$, and $C_{10}H_{22}$ molecules, respectively, while the dashed curve is the total number of the adsorbed monomers. Data is averaged over 50 ps.

IV. CONCLUSIONS

In conclusion, we study the selective adsorption in alkane mixtures and the adsorption-desorption dynamics around a CNT with MD simulations and master equation. Preferred adsorption of long chained molecules over short ones is found, which is attributed to the enhanced adsorption energy with more binding sites and less edge effects for the longer ones. Competing adsorptions and desorptions are through monomer by monomer processes. The broad and flat distribution in the morphology of the molecules with the bound fraction $f_b < 1$ is explained through the solution of a master equation for a saturated adsorption. A fully adsorbed alkane molecule is found to be more stable than a partially adsorbed one, with a much slower monomer desorption rate. The se-

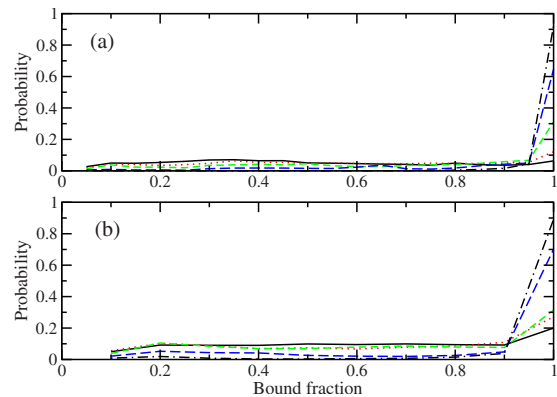


FIG. 8. (Color online) The (non-normalized) probability function for the adsorbed (a) $C_{20}H_{42}$ and (b) $C_{10}H_{22}$ molecules in the eicosane-decane mixture composite system at various temperatures during the cooling process (data averaged over 50 ps). Black solid, red (dark gray) dotted, green (gray) dashed, and blue (dark gray) long-dashed curve is for $T=590, 500, 400,$ and 300 K, respectively. The black dash-dotted curve is for $T=300$ K during a 10 ns extra simulation following the cooling process (data averaged over the last 1 ns).

lectivity and adsorption process is expected to be less influenced by the chirality and radius of the CNT than by the type of the polymer matrix. Crystallization of the mixture composites is also found during a cooling process from high to low temperatures, where selectivity of longer molecules over short ones and features in the molecule morphology with the domination of the much more stabled fully adsorbed state all present at the CNT surface in the wide temperature range.

ACKNOWLEDGMENT

This work is partially supported by NASA under Contract No. NAS2-03144 to UARC.

*chenyu.wei@nasa.gov

¹ *Carbon Nanotubes: Synthesis, Structure, Properties, and Applications*, edited by M. S. Dresselhaus, G. Dresselhaus, and P. Avouris (Springer, New York, 2000).

² See recent reviews in M. Moniruzzaman and K. Winey, *Macromolecules* **39**, 5194 (2006); J. N. Coleman, U. Khan, W. J. Blau, and Y. K. GunOk, *Carbon* **44**, 1624 (2006), and references there in.

³ M. A. C. Stuart, T. Cosgrove, and B. Vincent, *Adv. Colloid Interface Sci.* **24**, 143 (1985), and references there in.

⁴ Q. Zhang, D. R. Lippits, and S. Rastogi, *Macromolecules* **39**, 658 (2006).

⁵ F. H. J. Maurer, H. M. Schoffeleers, R. Kosfeld, and Th. Uhlenbroich, in *Progress in Science and Engineering of Composites*, Proceedings of the Fourth International Conference on Composite Materials, ICCM-IV, Tokyo, 1982, edited by T. Hayashi, K. Kawata, and S. Umekawa (North-Holland, Amsterdam, 1982), p. 803.

⁶ DLPOLY code from Daresbury Laboratory (UK) was used.

⁷ R. Czerw, Z. Guo, P. M. Ajayan, Y.-P. Sun, and D. L. Carroll, *Nano Lett.* **1**, 423 (2001); B. McCarthy, J. N. Coleman, R. Czerw, A. B. Dalton, M. in het Panhuis, A. Maiti, A. Drury, P. Bernier, J. B. Nagy, B. Lahr, H. J. Byrne, D. L. Carroll, and W. J. Blau, *J. Phys. Chem. B* **106**, 2210 (2002); H. Ago, R. Azumi, S. Ohshima, Y. Zhang, H. Kataura, and M. Yumura, *Chem. Phys. Lett.* **383**, 469 (2004); B. Philip, J. Xie, J. K. Abraham, and V. K. Varadan, *Smart Mater. Struct.* **13**, N105 (2004).

⁸ C. Wei, *Nano Lett.* **6**, 1627 (2006).

⁹ A. Nish, J.-Y. Hwang, J. Doig, and R. J. Nicholas, *Nat. Nanotechnol.* **2**, 640 (2007); F. Chen, B. Wang, Y. Chen, and L.-J. Li, *Nano Lett.* **7**, 3013 (2007).

¹⁰ M. Zheng, A. Jagota, M. S. Strano, A. P. Santos, P. Barone, S. G. Chou, B. A. Diner, M. S. Dresselhaus, R. S. Mclean, G. B. Onoa, G. G. Samsonidze, E. D. Semke, M. Usrey, and D. J. Walls, *Science* **302**, 1545 (2003).

¹¹ W. D. Cornell, P. Cieplak, C. I. Bayly, I. R. Gould, K. M. Merz,

- D. M. Ferguson, D. C. Spellmeyer, T. Fox, J. W. Caldwell, and P. A. Kollman, *J. Am. Chem. Soc.* **117**, 5179 (1995).
- ¹²C. Wei, D. Srivastava, and K. Cho, *Nano Lett.* **2**, 647 (2002).
- ¹³P. J. Flory, *Principles of Polymer Chemistry* (Cornell University, Ithaca, New York, 1995).
- ¹⁴Z. X. Xie, X. Xu, B. W. Mao, and K. Tankaka, *Langmuir* **18**, 3113 (2002).
- ¹⁵L. Messe, A. Perdigon, and S. M. Clarke, *Langmuir* **21**, 5085 (2005).
- ¹⁶T. K. Xia and U. Landman, *Science* **261**, 1310 (1993).
- ¹⁷S. P. Bates, W. J. M. van Well, R. A. van Santen, and B. Smit, *J. Am. Chem. Soc.* **118**, 6753 (1996); T. J. H. Vlught, R. Krishna, and B. Smit, *J. Phys. Chem. B* **103**, 1102 (1999); M. Schenk, S. L. Vidal, T. J. H. Vlught, B. Smit, and R. Krishna, *Langmuir* **17**, 1558 (2001); L. Lu, X. Lu, Y. Chen, L. Huang, Q. Shao, and Q. Wang, *Fluid Phase Equilib.* **259**, 135 (2007).
- ¹⁸A. J. Groszek, *Proc. R. Soc. London, Ser. A* **314**, 473 (1970).
- ¹⁹P. G. de Gennes, *Adv. Colloid Interface Sci.* **27**, 189 (1987).
- ²⁰P. Frantz and S. Granick, *Phys. Rev. Lett.* **66**, 899 (1991).
- ²¹K. R. Paserba and A. J. Gellman, *Phys. Rev. Lett.* **86**, 4338 (2001).
- ²²K. R. Paserba and A. J. Gellman, *J. Chem. Phys.* **115**, 6737 (2001).
- ²³Y. Wang, R. Rajagopalan, and W. L. Mattice, *Phys. Rev. Lett.* **74**, 2503 (1995).
- ²⁴K. A. Smith, M. Vladkov, and J.-L. Barrat, *Macromolecules* **38**, 571 (2005).
- ²⁵P. Frantz and S. Granick, *Macromolecules* **27**, 2553 (1994).
- ²⁶H. M. Schneider, P. Frantz, and S. Granick, *Langmuir* **12**, 994 (1996).
- ²⁷B. O'Shaughnessy and D. Vavylonis, *Phys. Rev. Lett.* **90**, 056103 (2003).
- ²⁸C. Wei, *Phys. Rev. B* **76**, 134104 (2007).